A Gravity Model for the Spread of a Pollinator-Borne Plant Pathogen

Matthew J. Ferrari,[1,*] Ottar N. Bjørnstad,[2,†] Jessica L. Partain,[3,‡] and Janis Antonovics[3,§]

1. Intercollege Graduate Degree Program in Ecology, Pennsylvania State University, University Park, Pennsylvania 16802;
2. Departments of Biology and Entomology, Pennsylvania State University, University Park, Pennsylvania 16802;
3. Department of Biology, University of Virginia, Charlottesville, Virginia 22904

Submitted June 16, 2005; Accepted June 14, 2006;
Electronically published July 26, 2006

ABSTRACT: Many pathogens of plants are transmitted by arthropod vectors whose movement between individual hosts is influenced by foraging behavior. Insect foraging has been shown to depend on both the quality of hosts and the distances between hosts. Given the spatial distribution of host plants and individual variation in quality, vector foraging patterns may therefore produce predictable variation in exposure to pathogens. We develop a "gravity" model to describe the spatial spread of a vector-borne plant pathogen from underlying models of insect foraging in response to host quality using the pollinator-borne smut fungus *Microbotryum violaceum* as a case study. We fit the model to spatially explicit time series of *M. violaceum* transmission in replicate experimental plots of the white campion *Silene latifolia*. The gravity model provides a better fit than a mean field model or a model with only distance-dependent transmission. The results highlight the importance of active vector foraging in generating spatial patterns of disease incidence and for pathogen-mediated selection for floral traits.

Keywords: gravity model, *Microbotryum*, *Silene*, spatial model, vector-borne pathogen.

A fundamental challenge in modeling the dynamics of infectious pathogens is specifying a model for the interaction among hosts in a population (McCallum et al. 2001). Conventional, population-level, susceptible-infected-removed-type epidemic models employ a mean field approximation that is an implicit model of complete population mixing. The functional form of mean field mixing models for host-pathogen systems is a subject of debate (Antonovics et al. 1995; Bucheli and Shykoff 1999; McCallum et al. 2001); the appropriate model depends on the transmission mechanism, the degree of heterogeneity in exposure, and the scaling of transmission with population size (Antonovics et al. 1995; McCallum et al. 2001). Network models of populations, in contrast, explore the effect of explicit social contact networks on epidemic dynamics (Newman 2002; Meyers et al. 2005). Such explicit networks can lead to very different predictions about pathogen invasion (Pastor-Satorras and Vespignani 2001, 2002) and evolution (Boots and Sasaki 1999; Read and Keeling 2003; Boots et al. 2004). By considering the underlying behavior that generates the contact networks, we propose a general model for characterizing the topology of the transmission network that incorporates both spatial interactions and host-specific heterogeneities in exposure.

The spread of disease in plant populations necessarily generates a spatial pattern in incidence as the hosts themselves are fixed in space. Analyzing the spatial distribution of disease incidence to make inference on transmission has become commonplace in plant pathogen systems (Campbell and Madden 1990; Real and McElhany 1996). Analyses using the observed pattern of spatial clustering to characterize a pathogen dispersal kernel are by necessity phenomenological (Mollison 1977; Campbell and Madden 1990). However, it is difficult to distinguish the process that generates a given pattern by characterizing the pattern alone (Real and McElhany 1996). Patchiness in disease incidence may signify either a spatially constrained transmission process or clustering of susceptibility due to environmental conditions or genetic relatedness (Campbell and Madden 1990). Conversely, the absence of clustering of incidence need not signify the lack of a contagious process.

Pathogens that are transmitted by arthropod vectors may exhibit spatial autocorrelation in incidence, but transmission may be further influenced by the foraging be-

* E-mail: mferrari@psu.edu.

† E-mail: onb1@psu.edu.

‡ E-mail: jlp3f@virginia.edu.

§ E-mail: ja8n@virginia.edu.

Am. Nat. 2006. Vol. 168, pp. 294–303. 0003-0147/2006/16803-41138$15.00.

havior of the vector (Real et al. 1992; Altizer et al. 1998). Considerable empirical and theoretical work has shown that foraging arthropods tend to make decisions about where to forage to maximize the rate of energy acquisition (Charnov 1976; Zimmerman 1981; Ohashi and Yahara 1999; Goulson 2000). Selective foraging by disease vectors, therefore, may result in differential exposure (Shykoff and Bucheli 1995; Shykoff et al. 1997) and infection rates (Alexander 1987; Thrall and Jarosz 1994) as a function of foraging quality, which in turn has implications for disease-induced selection on plant traits (Shykoff et al. 1997; Giles et al. 2005). In particular, vector-borne pathogens can result in selection against the host traits that attract vectors. Giles et al. (2005) showed strong directional selection for less attractive floral traits in *Silene dioica* as a result of the pollinator-borne anther smut *Microbotryum violaceum*. Similarly, pathogens are likely to influence selection on mating systems and monogamy in both plant and animal hosts (Thrall et al. 1997; Nunn et al. 2000).

In this article, we derive a "gravity model" for the spatial spread of a vector-borne pathogen from underlying models of insect movement and foraging behavior. We further discuss model fitting and predictions that allow an investigation of the relative contribution of spatial autocorrelation in transmission and vector choice in the generation of spatial patterns of infection. We develop these models using the pollinator-borne smut fungus *M. violaceum* as a case study.

A Gravity Model for Pathogen Exposure

By incorporating basic theory of vector foraging, we develop models that explicitly account for heterogeneities in pathogen exposure due to behavioral decisions. Insect foraging behavior in response to host plant spacing and quality has been extensively studied—both empirically and theoretically—in plant-pollinator systems (Charnov 1976; Ohashi and Yahara 1999, 2002; Goulson 2000). The exposure of a susceptible plant to a pollinator-borne pathogen is the result of three distinct processes: the acquisition of infectious particles by the vector from the infectious plant, the movement of the vector from the infectious to a susceptible plant, and the deposition of infectious particles on the susceptible plant. The rates associated with these three events are determined by the cumulative outcome of individual foraging decisions made by the population of vectors. In this way, the movement of pathogens between individuals or patches is similar to gene flow. Previous empirical studies have independently shown both separation distance and source and destination patch quality to influence the overall rate of gene flow between individuals and patches (Schmitt 1980; Ellstrand et al. 1989; Cresswell et al. 2002; Cresswell and Osborne 2004). We develop a general model of pathogen exposure for pollinator vector systems based on, first, the probability of movement between an infectious and susceptible plant as a function of distance and, second, the likelihood of spore transfer as a function of foraging duration on the infectious and susceptible plant hosts. The aggregate dynamics of transmission will be the result of many such individual moves by many pollinators. For simplicity, we consider only individual plant-to-plant moves by pollinators and ignore potential spore carryover along a sequence of multiple susceptible plants visited. Though developed in the context of pollinator systems, the framework should be generalizable to any system in which vectors actively select hosts on which to forage.

We first consider the probability of a pollinator moving between an infectious plant, i, and a susceptible plant, j, a distance d_{ij} away. Assuming that insect vectors have limited knowledge of plant quality before landing, we may model vector movement as a random walk (Broadbent and Kendall 1953; Okubo 1980). The resultant distribution of vector locations at time t will be Gaussian, with mean at the origin plant, i, and variance ωt, where ω is the diffusion constant and t is the transit time (Okubo 1980). Let the probability that the vector encounters a host plant during the random walk in any short interval δt be $\lambda \delta t$. Following Broadbent and Kendall (1953), the distribution of vectors on a circle of radius r, centered at the origin plant, is then

$$f(r) = \frac{r}{\alpha^2} K_0\left(\frac{r}{\alpha}\right), \tag{1}$$

where $\alpha = 1/(2\lambda/\omega)^{1/2}$ and $K_0(\cdot)$ is a modified Bessel function of order 0. To obtain the distribution of moves between two specific plants separated by a distance d_{ij} (i.e., from one plant to another plant on the circle), we take the average over the circumference to obtain

$$f(d_{ij}) = \frac{1}{2\pi\alpha^2} K_0\left(\frac{d_{ij}}{\alpha}\right). \tag{2}$$

Thus, the probability of a move between an infectious plant i and a susceptible plant j is a decreasing function of their distance apart and depends on the diffusion rate according to the parameter α.

Conditional on the move between them, the acquisition of spores from an infectious host and the deposition of spores on a susceptible host are similar processes in that they are related to the number of flowers visited on the host plant. Pollinator foraging intensity is greatly influenced by the number of flowers open at any one time on a plant (floral display). Pollinators seeking to maximize

net energy gain should spend relatively more time visiting plants with larger floral displays (Charnov 1976; Goulson 2000; Ohashi and Yahara 2002). When those pollinators are also vectors of a pathogen, increased foraging intensity will translate into increased pathogen exposure (Shykoff and Bucheli 1995; Shykoff et al. 1997). By considering the relationship between floral display size and the duration of foraging bouts, we can derive a functional form for the effect of floral display on pathogen exposure. It should be easily generalized to any vector-borne system in which some measure of host quality is substituted for floral display size.

From Charnov's (1976) "marginal value theorem," a forager should leave a patch when the rate of resource acquisition falls below the region-wide mean. Ohashi and Yahara (1999) studied a stochastic, discrete analog of this theory that applies to a pollinator foraging on individual flowers on a plant. Assuming the pollinator visits flowers at random, the probability of encountering a previously depleted flower increases with the number of flowers probed and decreases with the total number of flowers on the plant, F_{Tot}. The risk of encountering a depleted flower will increase with time spent foraging (i.e., flowers visited). Weighing this risk against the discounting rate, k, for visiting any flower on other plants—that is, $k = [(\text{flight time per flower within a plant}) + (\text{handling time per flower})]/[(\text{flight time between plants}) + (\text{handling time per flower})]$—Ohashi and Yahara (1999) showed that the optimal number of flowers to visit, F^*, is linearly related to the total number of flowers on a plant:

$$F^* \approx (1 - k)F_{\text{Tot}}. \tag{3}$$

Given that a forager moves from plant i to j and forages according to the optimal rule, we can calculate the spore deposition on plant j as a function of the total number of flowers, F_{Tot}. Assuming that spore deposition decreases exponentially as flowers on an individual plant are visited (for empirical support of this assumption, see Altizer et al. 1998), we then write the number of spores deposited per flower, S, as

$$S = \xi e^{-\phi x}, \tag{4}$$

where ξ is proportional to the number of spores carried from host i by the vector, ϕ is the discounting rate, and x is the flower number in a visitation sequence. Integrating equation (4), we obtain the total spore deposition, S_{Tot}, for a pollinator visiting F flowers on a plant:

$$\begin{aligned} S_{\text{Tot}} &= \int_0^F \xi e^{-\phi x} dx \\ &= \frac{\xi}{\phi}(1 - e^{-\phi F}). \end{aligned} \tag{5}$$

Substituting the optimal flower number (eq. [3]) into equation (5), we obtain

$$S_{\text{Tot}} = \frac{\xi}{\phi}[1 - e^{-\phi(1-k)F_{\text{Tot}}}],$$

which is approximately

$$S_{\text{Tot}} \approx \xi(1 - k)F_{\text{Tot}} \tag{6}$$

when $\phi(1 - k)F_{\text{Tot}}$ is small. This approximation is good whenever the decay rate in spore deposition is slow ($\phi < 0.5$) and the cost of interplant movement is low ($k > 0.5$).

Recalling that ξ is proportional to the number of spores carried by the vector from infectious host i and assuming that the vector accumulates spores at a rate γ during the course of foraging within a plant, then the spores acquired is a function of the total number of flowers according to

$$\xi = \gamma(1 - k)F_{\text{Tot}}. \tag{7}$$

Note that equation (7) assumes that all flowers on plant i are infectious (i.e., the infection is systemic). This is not necessarily the case for pollinator-borne pathogens (e.g., *Microbotryum violaceum* discussed below), for which plants may exhibit partial infection. In such cases, equation (7) may be altered to reflect the number of infectious flowers (see "Case Study: *Silene latifolia* and *Microbotryum violaceum*").

Combining equations (6) and (7), we can write the total flow of spores from infectious plant i to susceptible plant j as

$$\gamma\delta(1 - k)^2 F_{\text{Tot},i} F_{\text{Tot},j}, \tag{8}$$

where $F_{\text{Tot},i}$ and $F_{\text{Tot},j}$ are the total flowers on plants i and j, respectively.

For a given spore exposure (eq. [8]), we assume a Poisson dose response relationship to give the probability of an effective transmission from i to j as

$$P_{ij} = 1 - \exp(-\tau F_{\text{Tot},i} F_{\text{Tot},j}), \tag{9}$$

where $\tau = \gamma\delta(1 - k)^2$. Note that we assume that the deposition of spores from plant i on plants visited after j is

negligible, and so the probability of transmission can thus be characterized in terms of this pairwise interaction.

Combining the probabilities of exposure as a function of distance (eq. [1]) and as a function of floral display sizes (eq. [9]), and scaling by the spore intensity θ, we arrive at the "gravity" model of exposure

$$E_{ij} = \theta[1 - \exp(-\tau F_{\text{Tot},i} F_{\text{Tot},j})] \frac{K_0(d_{ij}/\alpha)}{2\pi\alpha^2}. \quad (10)$$

Gravity models have been used to describe spatial interaction models with site-specific effects in economics (Fitzsimons et al. 1999), transportation (Erlander and Stewart 1990), demography (Murray and Cliff 1977), ecology (Bossenbroek et al. 2001), and epidemiology (Murray and Cliff 1977; Xia et al. 2004). The unifying characteristic of these models is that the strength of interaction between sites (populations, locations, or individuals) is bilinear in some site variable and decays as a function of the distance between sites (Bailey and Gatrell 1995). In this way, the models are analogous to gravitational attraction between planetary bodies.

The total exposure of any susceptible plant, *j*, is consequently given by the sum of the exposure to all infectious plants:

$$E_j = \sum_{\substack{i \in \text{infected} \\ j \in \text{susceptible}}} \theta[1 - \exp(-\tau F_{\text{Tot},i} F_{\text{Tot},j})] \frac{K_0(d_{ij}/\alpha)}{2\pi\alpha^2}. \quad (11)$$

Importantly, there are three relevant submodels contained within the gravity model. Setting the term containing $F_{\text{Tot},i}$ and $F_{\text{Tot},j}$ to 1, that is, equation (9), equation (11) reduces to a purely distance-based model of transmission. We will call this submodel the distance-decay model (DD). Setting the term containing d_{ij} to 1, that is, equation (2), equation (11) reduces to a function only of the floral displays; we call this the host-quality model (HQ). Last, setting the second and third terms in equation (11) to 1, the model reduces to the common density-dependent, mean field model (McCallum et al. 2001).

Parameter Estimation

Direct observation of pathogen flow between individuals is difficult. Therefore, to make the above models applicable to real data, we must consider a statistical model with observable data as inputs; while we cannot usually observe the transfer of infectious spores, we can often make observations of the change in distribution of infected plants over time. Assuming that the probability of an individual becoming infected at any given time is a function of its level of exposure, we can develop a statistical model based on the timing of infection.

Considering the simplest case, where infection is permanent and nonfatal, we denote the status of host j at time t, $X_{j,t}$, as 0 if the host is susceptible and 1 if it is infected. Assuming that infection is a Poisson process in time, with rate parameter determined by the exposure to spores, we write the probability that the susceptible host j is infected after a time step δt as

$$P_{j,\delta t} = 1 - \exp(-E_j \delta t). \quad (12)$$

It is then straightforward to write the binomial likelihood for infection status of host j given the probability $P_{j,\delta t}$ (for ease of notation, we will consider only time steps of length 1). We employ a discrete time Markov assumption, which states that the status of any plant at time $t + 1$ depends on the distribution of infection at the previous time step and that all hosts are conditionally independent (for methods when the Markov assumption is inappropriate, see Gibson 1997). We then write the joint likelihood for the observed distributions of infection for N individuals sampled at T discrete time intervals as the product of the individual likelihoods:

$$L(P|X_t) = \prod_{t=1}^{T-1} \prod_{j=1}^{N} (P_{j,t})^{X_{j,t}} (1 - P_{j,t})^{1 - X_{j,t}}, \quad (13)$$

where $P_{j,t}$ is given by equations (11) and (12). Maximizing over equation (13), we obtain estimates of the parameters of the exposure model. We apply model selection criteria from likelihood theory (e.g., likelihood ratios, Akaike Information Criterion [AIC]) to choose the best among candidate submodels (McCullagh and Nelder 1989).

Simulation Experiments

We evaluated the ability of the statistical framework to distinguish among the DD, HQ, and gravity (GR) exposure models using data generated by simulation. We simulated 60 spatial epidemics on an 8 × 8 lattice of hosts at each of nine factorial combinations of weak, medium, and strong levels of distance effects ($\alpha = 1$, 5, and 10 in eq. [4]) and host quality effects ($\tau = 0.01$, 0.05, and 1.0 in eq. [11]; fig. 1). These parameter levels were chosen such that the extremes ($\alpha = 10$ and $\tau = 1.0$) should resemble the HQ and DD models, respectively. For a given spore production rate, the different parameter combinations for α and τ result in different rates of infection at the plot level. To control the plot level infection rate, we scaled the spore production rate, θ, to give constant plot level force of infection for each parameter combination.

We generated simulations using a spatially extended ver-

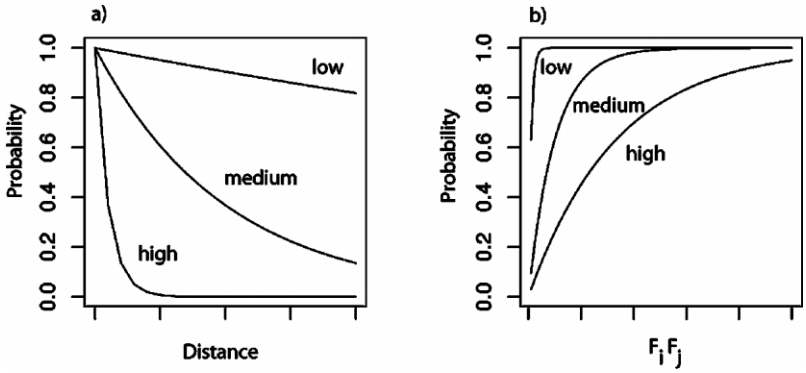

Figure 1: Probability of spore transmission from host i to j as a function of (a) distance and (b) floral display (F) for the parameter values used in the simulation model.

sion of the epidemic birth and death model. Hosts were initialized with random floral displays that varied in time according to a random walk. Following standard theory (Renshaw 1991), waiting times to infection were drawn for each susceptible host from an exponential distribution, with rate determined by the exposure from the gravity model (eq. [11]). In accordance with the Gillespie algorithm, time was incremented forward, and new exposure weights were calculated following each event. This process was repeated until all hosts were infected. This spatial epidemic birth and death model generates realizations of the epidemic process in continuous time. Observation of a spatial epidemic, in contrast, is usually in discrete time. To mirror such an observation process, the distribution of susceptible and infected individuals was "observed" every 10 time units. Thus, multiple chains of infection between observations were possible.

We fit the DD, HQ, and GR models to the observed time series for each simulation by maximizing the likelihood given in equation (13). We then selected the best fit model using corrected AIC (AIC_c). The nonspatial, null model was rejected in all simulations at all parameter combinations. As expected, the full gravity model tended to be selected as the best fit when the distance and host quality effects were of similar magnitude (i.e., both medium or both large; fig. 2). When the parameter combination included a stronger effect of either distance or host quality, the appropriate simpler model was more often selected. In the extreme limit, when both the distance and host quality effects were small, model selection was highly variable.

For a given simulation run, the maximum likelihood estimates of the distance and host quality parameters for the best fit model tended to reflect the true parameter values when the effect sizes were large (i.e., α and τ small; fig. 3). When the effect sizes were small (i.e., α and τ large), the maximum likelihood estimates tended to be biased toward 0. Note, though, that the simpler submodels were usually favored for the latter parameter combinations. When one of the submodels (DD or HQ) was selected as best fit, the parameter estimates were more consistent over the full parameter range, though with a tendency toward a positive bias (fig. 3).

Case Study: *Silene latifolia* and *Microbotryum violaceum*

Microbotryum violaceum, or anther smut disease, is a fungal pathogen that commonly infects members of the Caryophyllaceae such as *Silene latifolia* (white campion), a

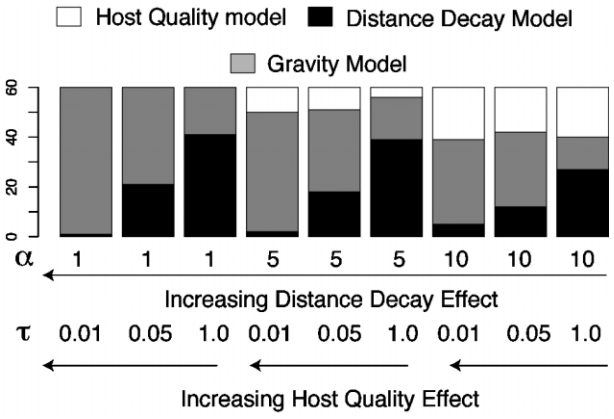

Figure 2: Results of model selection on simulated epidemics. The shaded bars indicate the number of simulations, out of 60, for which the gravity, distance decay, and host quality models were selected at each of nine parameter combinations. Numbers underneath each bar indicate the value of the distance decay parameter (α) and the host quality parameter (τ). Arrows give the qualitative effects of the parameter combinations.

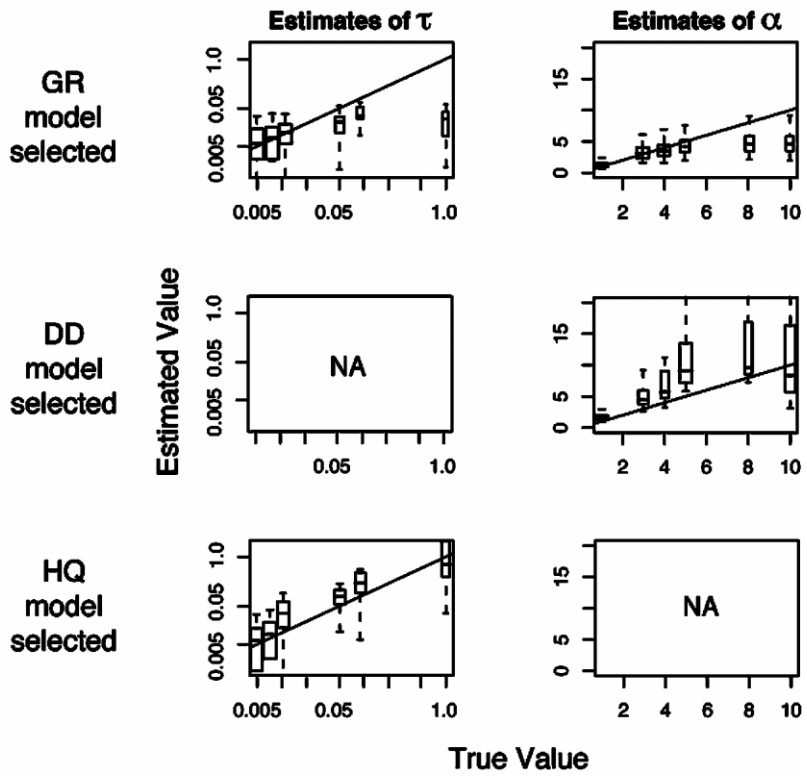

Figure 3: Parameter estimates for simulation experiments. The rows indicate model runs in which the gravity, distance decay, and host quality models were selected as the best fit. Columns indicate estimates of the host quality parameter (τ) and distance decay parameter (α). Each panel gives the estimated parameter values as a function of the true value used in the simulation. Box plots indicate the median and interquartile range; dashed lines indicate the most extreme estimate no more than 1.5 times the interquartile range from the box. Solid lines indicate estimated value = true value.

short-lived, dioecious perennial that generally occurs along roadsides and other semidisturbed habitats. When infected, both male and female plants produce spore-bearing anthers and are completely sterilized. The infection is spread via pollinators such as bumblebees and various moth species (Altizer et al. 1998), and the latent period of infection is approximately 3–4 weeks (Alexander and Antonovics 1988). In Virginia, natural populations of *S. latifolia* flower between late May and late October, and this long flowering season can allow more than one cycle of transmission.

Previous studies have shown distance effects in fungal spore deposition (Altizer et al. 1998) and increased infection risk for individuals with larger floral displays (Alexander 1987; Thrall and Jarosz 1994; Shykoff and Bucheli 1995; Shykoff et al. 1997). However, these effects have not previously been explored using a spatially explicit model at the individual level. In 1999, Antonovics et al. (2002) set up three replicate experimental populations of *S. latifolia*. Each population consisted of 64 individuals, arranged in an 8 × 8 grid with 0.75-m spacing. Of these, 14 plants were lab-inoculated "sources" of the infection, and the remaining 50 plants were healthy "target" plants. Individuals were subsequently monitored at weekly intervals to record the growth form of the plant as vegetative or flowering (some individuals spend the season as a nonflowering rosette), the disease status (healthy or diseased), and the numbers of healthy and diseased flowers. Data were collected for 19 weeks from June 12, 1999, to October 22, 1999.

During their first season, individuals that have been infected generally exhibit partial infection (i.e., they produce both normal and spore-bearing flowers). As such, an infected plant can, at any given observation point, have no spore-bearing flowers. In our analysis, we considered plants as infected for all time points after the first observation of a spore-bearing flower (i.e., disease status as a binary variable, healthy or diseased). However, to account for the partial infection, we modified the HQ and GR models so that they reflected the observed number of spore-bearing flowers per infectious host. Because of the long latent period, the floral display at the onset of symp-

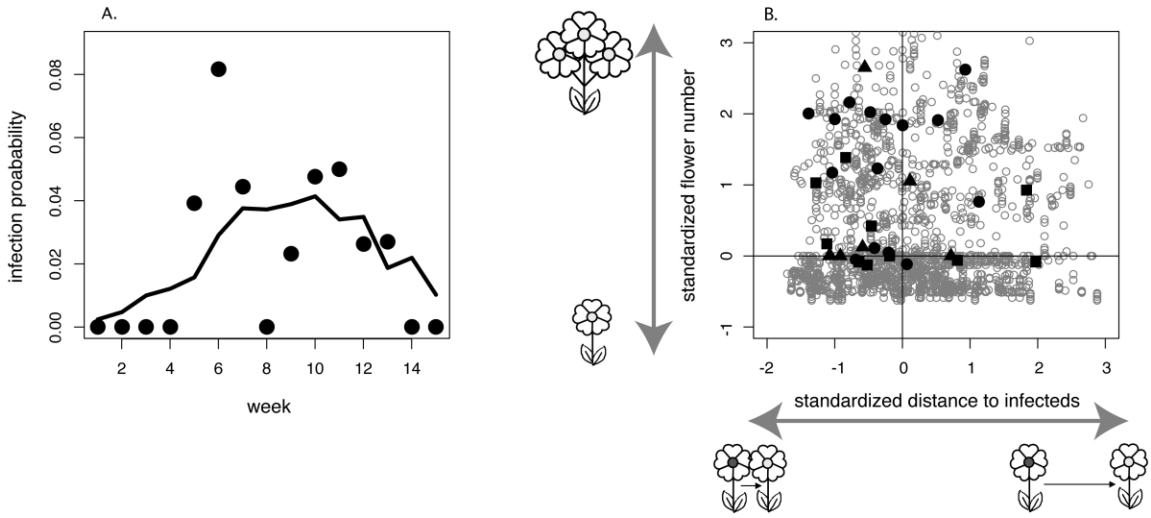

Figure 4: *A*, Observed (*circles*) and predicted (*line*) infection probability over time for the gravity model fitted to replicate A. Observed infection probability is the proportion of susceptible plants infected per week. *B*, Relative floral display size and distance to infected plants of *S. latifolia* individuals that became infected. For each observation point, the sum of the distances of each susceptible plant to all infected plants (*X*-axis) and the number of flowers (*Y*-axis) per plant are plotted. Values are standardized relative to the median and variance at the time of observation. Thus, the upper left quadrant indicates plants that were larger than average and closer to infected hosts than average. Filled symbols indicate observations of transitions from susceptible to infected status, lagged by the 3-week latent period (i.e., the conditions when they were likely to have been infected): *circle*, replicate A; *triangle*, replicate B, *square*, replicate C. Open gray circles indicate susceptible plants that remained susceptible. All observation points for all plants in three replicates are plotted.

toms may not reflect the conditions at the time of infection. To correct for this, we used 3-week time lagged flower counts. We fit the four competing models to the weekly incidence and flowering data for the three replicates.

Overall, the pattern of infection in all plots supports significant effects of both distance and a floral display (fig. 4). Of all infected plants, 47% both were relatively closer to infectious hosts and had relatively larger floral displays at the time of infection; 87% were either closer or larger than average (fig. 4). Our gravity model was strongly supported in replicate A (table 1). The gravity model provided a good fit to the infection rates through time for replicate A (fig. 4*A*). Within any given week, there was significant variation in the predicted probability of infection as a function of individual variation in floral display and spatial location; in general, infections occurred among plants that were larger and/or closer to infected sources than expected by chance (fig. 4*B*). The HQ model was selected as the best fit model in replicate C (table 1). The estimated host quality parameter, τ, was similar in magnitude for replicates A and C, suggesting a similar effect of floral display size on infection risk. The gravity model was weakly selected as the best fit model in replicate B ($\Delta AIC_c < 1$), though the parameter values suggest little effect of distance or floral display. The fact that the null model was not selected may reflect the fact that plants with 0 flowers never become infected; that is, the null model assumes that nonflowering plants can be infected.

The finding that models incorporating floral display were better supported than the null or distance-dependent model is consistent with previous studies of the *Silene-Microbotryum* system. Shykoff and Bucheli (1995) found higher rates of fluorescent dye deposition on *S. latifolia* individuals with larger floral display sizes. Further, Alexander (1987) and Thrall and Jarosz (1994) showed, using different experimental populations of *S. latifolia*, that individuals that produced large numbers of flowers over the course of the growing season were more likely to become infected. The gravity model we have presented may thus be seen as a synthesis of the previous experimental results in this spatially explicit system.

That the gravity model was relatively less supported in replicates B and C may reflect either that the number of infections (7 and 11 compared with 15 in replicate A) was too small to provide sufficient power to differentiate between models or that the spatial scale of the experimental design was too small and the temporal scale of observation too long to detect these effects. While both may have contributed, the latter seems likely to be important because the model was developed after the experiment had been designed and implemented. From the model formulation above, we predict that the strength of the distance effect

Table 1: Results of model fitting for the spread of *Microbotryum* in experimental plots of *Silene latifolia*

Plot and model	ΔAIC_c	Parameter estimates		
		θ	α	τ
A (15):				
Null	31	.023	…	…
Distance	27	.131	1.25	…
Host quality	4	.004	…	4.50
Gravity	…	**.759**	**1.02**	**.42**
B (7):				
Null	9	.010	…	…
Distance	9	.287	8.95	…
Host quality	.1	.002	…	4.50
Gravity	…	**1.774**	**21**	**9.98**
C (11):				
Null	25	.015	…	…
Distance	20	.108	.96	…
Host quality	…	**.004**	…	**.65**
Gravity	.05	7.144	81	.65

Note: Parameters θ, α, and τ are the scaling, distance, and host quality parameters, respectively. Number in parentheses gives the number of infections in each plot. AIC_c = corrected Akaike Information Criterion. For each plot, the best fit model and the corresponding parameter estimates are given in bold.

will diminish if the vectors are highly mobile relative to the scale of observation. Natural populations of *Silene* tend to occur in patches along roadsides, and the scale of this experiment replicated the within-patch scale. It would be interesting in the future to compare the dynamics of infection between patches, where the effect of spatial distance is more likely to be important.

Discussion

Though epidemics are classically studied at the population scale, the dynamics of transmission often involve the behavior of individual hosts or vectors. The mean field models for transmission dynamics based on mass-action kinetics have been very successful in describing a broad sample of both vector-borne and directly transmitted pathogens (Anderson and May 1991; Antonovics et al. 1995; McCallum et al. 2001). Increasingly, however, the importance of heterogeneities in transmission due to individual characteristics has been recognized to have important consequences for the dynamics of epidemics (Real et al. 1992). Recent network models of epidemic spread have illustrated how variation in the number of contacts between hosts can impact the threshold conditions for pathogen invasion (Andersson 1997; May and Lloyd 2001; Eames and Keeling 2002) and the evolution of virulence (Read and Keeling 2003; Boots et al. 2004). While these heterogeneities are generally recognized in many systems, they are often elusive to measure. In this article, we have presented a gravity model for the heterogeneities in exposure that result from the foraging behavior of disease vectors and spatial location of infection. Further, we have developed a statistical framework for evaluating the relative importance of such heterogeneities versus spatial effects using spatially explicit time series on the distribution of infection.

Given that vectors tend to forage actively and that the spatial arrangement of hosts will influence the order of contact, one would expect the true biological dynamics of exposure to incorporate both host quality and spatial components, as reflected in our gravity model. The degree to which the full gravity model is necessary to describe the observed dynamics of pathogen spread will certainly depend on the specific system and the scale of observation. In the *Silene* case study, host floral characteristics were consistently important in determining pathogen spread, and spatial effects were sometimes important. Had the experimental plots been larger, a different result might have been obtained. From the gravity formulation, we may expect the spatial scale of the transmission dynamics to be a function of both the movement abilities of the vectors and the heterogeneity in host characteristics. As host variation increases, it will become advantageous for the vectors to make larger moves between high quality hosts. In the *Silene* example, floral displays vary from 0 (i.e., no reward to pollinators) to 70 flowers, which represents a very large range of pollinator rewards. Given the mobility of the pollinators, it is not surprising that the spatial effect tended to be weak, because the variation in host quality likely imposes a spatial scale greater than the experimental scale. Interestingly, any spatial autocorrelation in host quality—for instance, due to clumping of host genotypes or environmental conditions—should result in a reduction in the spatial scale of transmission and perhaps lower overall levels of transmission; Biere and Antonovics (1996) found marginally reduced transmission rates in experimental plots of *Silene latifolia* where host genotypes were clumped compared with randomly distributed.

Increased pathogen exposure due to floral display size will have strong implications for the evolution of reproductive allocation and vector/pollinator-mediated selection on host reproductive traits. Interestingly, field observation has repeatedly shown that plants with smaller floral displays are overrepresented in populations resistant to *Microbotryum violaceum* (Alexander 1989; Biere and Antonovics 1996; Giles et al. 2005). Giles et al. (2005) recently documented directional selection on traits affecting female attractiveness in *Silene dioica* as a result of infection by *M. violaceum*. This pollinator-mediated selection highlights the trade-off between allocation to reproduction (size and quality of floral display) and survival and/or

future reproductive success, given the risks of pathogen infection. The gravity model for transmission can make explicit the dependence of the strength of pollinator-mediated selection on the spatial scale of vector movement and the variation in host traits. Such a trade-off is not necessarily restricted to pollinator systems and may be applicable to any pathogen system in which sexual display or promiscuity increases both fitness and pathogen exposure. The trade-off will be particularly strong in other sexually transmitted diseases. Using individual-based models, Thrall et al. (1997) showed that sexually transmitted (and sterilizing) pathogens can have significant impacts on host mating behavior. Paralleling this, Nunn et al. (2000) found higher white blood cell counts in primate species where females have many mating partners, suggesting increased pathogen exposure due to promiscuity and, as a consequence, a selective pressure for monogamous mating systems.

The idea of gravity-like dynamics describing the interaction of spatially distinct population units is intuitive, given that organisms tend to be choosy about their choice of location for feeding, mating, oviposition, and so on. Gravity models have previously been used to describe the flow of humans between population centers (Murray and Cliff 1977; Erlander and Stewart 1990). Here we have presented a very specific functional form for the interaction strength between two hosts derived from models of insect movement and foraging decisions. However, it is quite possible that a more generic and phenomenological formulation for the interaction (E_{ij}), of the form $E_{ij} \propto (X_i^{\alpha} X_j^{\beta} / d_{ij}^{\gamma})$—where X_i is some host trait of host attractiveness; d_{ij} is a measure of distance between host i and j; and α, β, and γ are tuning parameters—would still be instructive for systems where the movement behavior of the vectors is less well known. This generic model was recently used to describe the risk of measles outbreaks in Britain in the prevaccination era; there, X was taken to be equal to population size of municipalities (Xia et al. 2004). It has also been used for the invasion of zebra mussels to inland lakes, in which case X was related to the relative recreational fishing traffic (Bossenbroek et al. 2001). Moreover, Cresswell and Osborne (2004) describe the flow of pollen between patches of oilseed rape as dependent on both patch size and spatial separation, and De Moraes and coauthors (De Moraes et al. 1998; De Moraes and Mescher 1999) have documented directed movement of organisms, particularly insects, in response to plant volatile compounds or conspecific pheromones that are induced in response to host quality and infestation levels. Much of the classic work in spatial population dynamics has assumed that dispersal is isotropic or anisotropic with a consistent bias. Here we have shown both theoretical and empirical evidence for biased pathogen dispersal in response to dynamic patch/host quality. The resultant gravity dynamics in spatial interactions may have important implications for evolution and stability of spatial population dynamics and may warrant further investigation.

Literature Cited

Alexander, H. M. 1987. Pollination limitation in a population of *Silene alba* infected by the anther smut fungus, *Ustilago violacea*. Journal of Ecology 75:771–780.

———. 1989. An experimental field study of anther smut disease of *Silene alba* caused by *Ustilago violacea*: genotypic variation and disease incidence. Evolution 43:835–847.

Alexander, H. M., and J. Antonovics. 1988. Disease spread and population dynamics of anther smut infection of *Silene alba* caused by the fungus *Ustilago violacea*. Journal of Ecology 76:91–104.

Altizer, S. M., P. H. Thrall, and J. Antonovics. 1998. Vector behavior and the transmission of anther smut infection in *Silene alba*. American Midland Naturalist 139:147–163.

Anderson, R. M., and R. M. May. 1991. Infectious diseases of humans: dynamics and control. Oxford University Press, Oxford.

Andersson, H. 1997. Epidemics in a population with social structures. Mathematical Biosciences 140:79–84.

Antonovics, J., Y. Iwasa, and M. P. Hassell. 1995. A generalized model of parasitoid, venereal, and vector-based transmission processes. American Naturalist 145:661–675.

Antonovics, J., M. Hood, and J. Partain. 2002. The ecology and genetics of a host shift: *Microbotryum* as a model system. American Naturalist 160(suppl.):S40–S53.

Bailey, T. C., and A. C. Gatrell. 1995. Interactive spatial data analysis. Wiley, New York.

Biere, A., and J. Antonovics. 1996. Sex-specific costs of resistance to the fungal pathogen *Ustilago violacea* (*Microbotryum violaceum*) in *Silene alba*. Evolution 50:1098–1110.

Boots, M., and A. Sasaki. 1999. "Small worlds" and the evolution of virulence: infection occurs locally and at a distance. Proceedings of the Royal Society of London B 266:1933–1938.

Boots, M., P. J. Hudson, and A. Sasaki. 2004. Large shifts in pathogen virulence relate to host population structure. Science 303:842–844.

Bossenbroek, J. M., C. E. Kraft, and J. C. Nekola. 2001. Prediction of long-distance dispersal using gravity models: zebra mussel invasion of inland lakes. Ecological Applications 11:1778–1788.

Broadbent, S. R., and D. G. Kendall. 1953. The random walk of *Trichostrongylus retortaeformis*. Biometrics 9:460–464.

Bucheli, E., and J. A. Shykoff. 1999. The influence of plant spacing on density-dependent versus frequency-dependent spore transmission of the anther smut *Microbotryum violaceum*. Oecologia (Berlin) 119:55–62.

Campbell, C. L., and L. V. Madden. 1990. Introduction to plant disease epidemiology. Wiley, New York.

Charnov, E. L. 1976. Optimal foraging: the marginal value theorem. Theoretical Population Biology 9:126–136.

Cresswell, J. E., and J. L. Osborne. 2004. The effect of patch size and separation on bumblebee foraging in oilseed rape: implications for gene flow. Journal of Applied Ecology 41:539–546.

Cresswell, J. E., J. L. Osborne, and S. A. Bell. 2002. A model of pollinator-mediated gene flow between plant populations with numerical solutions for bumblebees pollinating oilseed rape. Oikos 98:375–384.

De Moraes, C. M., and M. C. Mescher. 1999. Interactions in ento-

mology: plant-parasitoid interaction in tritrophic systems. Journal of Entomological Science 34:31–39.

De Moraes, C. M., W. J. Lewis, P. W. Pare, H. T. Alborn, and J. H. Tumlinson. 1998. Herbivore-infested plants selectively attract parasitoids. Nature 393:570–573.

Eames, K. T. D., and M. J. Keeling. 2002. Modeling dynamic and network heterogeneities in the spread of sexually transmitted diseases. Proceedings of the National Academy of Sciences of the USA 99:13330–13335.

Ellstrand, N. C., B. Devlin, and D. L. Marshall. 1989. Gene flow by pollen into small populations: data from experimental and natural stands of wild radish. Proceedings of the National Academy of Sciences of the USA 86:9044–9047.

Erlander, S., and N. F. Stewart. 1990. The gravity model in transportation analysis—theory and extensions. International Science, Utrech.

Fitzsimons, E., V. Hogan, and J. P. Neary. 1999. Explaining the volume of North-South trade in Ireland: a gravity model approach. Economic and Social Review 30:381–401.

Gibson, G. J. 1997. Markov chain Monte Carlo methods for fitting spatiotemporal stochastic models in plant epidemiology. Applied Statistics 46:215–233.

Giles, B. E., T. M. Pettersson, U. Carlsson-Graner, and P. K. Ingvarsson. 2005. Natural selection on floral traits of female *Silene dioica* by a sexually transmitted disease. New Phytologist 169:637–640.

Goulson, D. 2000. Why do pollinators visit proportionally fewer flowers in large patches? Oikos 91:485–492.

May, R. M., and A. L. Lloyd. 2001. Infection dynamics on scale-free networks. Physical Review E 64:066112.

McCallum, H., N. Barlow, and J. Hone. 2001. How should pathogen transmission be modelled? Trends in Ecology & Evolution 16:295–300.

McCullagh, P., and J. A. Nelder. 1989. Generalized linear models: monographs on statistics and applied probability. Vol. 37. Chapman & Hall, London.

Meyers, L. A., B. Pourbohloul, M. E. J. Newman, D. M. Skowronski, and R. C. Brunham. 2005. Network theory and SARS: predicting outbreak diversity. Journal of Theoretical Biology 232:71–81.

Mollison, D. 1977. Spatial contact models for ecological and epidemic spread. Journal of the Royal Statistical Society B 39:283–326.

Murray, G. D., and A. D. Cliff. 1977. A stochastic model for measles epidemics in a multi-regional setting. Transactions of the Institute of British Geographers 2:158–174.

Newman, M. E. J. 2002. Spread of epidemic disease on networks. Physical Review E 66:016128.

Nunn, C. L., J. L. Gittleman, and J. Antonovics. 2000. Promiscuity and the primate immune system. Science 290:1168–1170.

Ohashi, K., and T. Yahara. 1999. How long to stay on, and how often to visit a flowering plant? a model for foraging strategy when floral displays vary in size. Oikos 86:386–392.

———. 2002. Visit larger displays but probe proportionally fewer flowers: counterintuitive behaviour of nectar-collecting bumble bees achieves an ideal free distribution. Functional Ecology 16: 492–503.

Okubo, A. 1980. Diffusion and ecological problems: mathematical models. Springer, Berlin.

Pastor-Satorras, R., and A. Vespignani. 2001. Epidemic spreading in scale-free networks. Physical Review Letters 86:3200–3203.

———. 2002. Epidemic dynamics in finite size scale-free networks. Physical Review E 65:035108.

Read, J. M., and M. J. Keeling. 2003. Disease evolution on networks: the role of contact structure. Proceedings of the Royal Society of London B 270:699–708.

Real, L. A., and P. McElhany. 1996. Spatial pattern and process in plant-pathogen interactions. Ecology 77:1011–1025.

Real, L. A., E. A. Marshall, and B. M. Roche. 1992. Individual behavior and pollination ecology: implications for the spread of sexually transmitted plant diseases. Pages 492–508 *in* D. L. De Angelis and L. J. Gross, eds. Individual based models and approaches in ecology. Chapman & Hall, New York.

Renshaw, E. 1991. Modelling biological populations in space and time: Cambridge studies in mathematical biology. Vol. 11. Cambridge University Press, Cambridge.

Schmitt, J. 1980. Pollinator foraging behavior and gene dispersal in *Senecio* (Compositae). Evolution 34:934–943.

Shykoff, J. A., and E. Bucheli. 1995. Pollinator visitation patterns, floral rewards and the probability of transmission of *Microbotryum violaceum*, a venereal disease of plants. Journal of Ecology 83:189–198.

Shykoff, J. A., E. Bucheli, and O. Kaltz. 1997. Anther smut disease in *Dianthus silvester* (Caryophyllaceae): natural selection on floral traits. Evolution 51:383–392.

Thrall, P. H., and A. M. Jarosz. 1994. Host-pathogen dynamics in experimental populations of *Silene alba* and *Ustilago violacea*. 1. Ecological and genetic determinants of disease spread. Journal of Ecology 82:549–559.

Thrall, P. H., J. Antonovics, and J. D. Bever. 1997. Sexual transmission of disease and host mating systems: within-season reproductive success. American Naturalist 149:485–506.

Xia, Y. C., O. N. Bjornstad, and B. T. Grenfell. 2004. Measles metapopulation dynamics: a gravity model for epidemiological coupling and dynamics. American Naturalist 164:267–281.

Zimmerman, M. 1981. Optimal foraging, plant density and the marginal value theorem. Oecologia (Berlin) 49:148–153.

Associate Editor: Matthew J. Keeling
Editor: Donald L. DeAngelis